Rapid Communications

Bright, continuous beams of cold free radicals

J. C. Shaw and D. J. McCarron*

Department of Physics, University of Connecticut, 196 Auditorium Road, Unit 3046, Storrs, Connecticut 06269, USA

(Received 3 August 2020; accepted 16 September 2020; published 21 October 2020)

We demonstrate a cryogenic buffer gas-cooled molecular beam source capable of producing bright, continuous beams of cold and slow free radicals via laser ablation over durations of up to 60 seconds. The source design uses a closed liquid helium reservoir as a large thermal mass to minimize heating and ensure reproducible beam properties during operation. Under typical conditions, the source produces beams of our test species SrF, containing 5×10^{12} molecules per steradian per second in the $X\,^2\Sigma(v = 0, N = 1)$ state with a rotational temperature of 1.0(2) K and a forward velocity of 140 m/s. The beam properties are robust and unchanged for multiple cell exit geometries, but depend critically on the helium buffer gas flow rate, which must be $\geqslant$10 standard cubic centimeters per minute to produce bright, continuous beams of molecules for an ablation repetition rate of 55 Hz.

DOI: 10.1103/PhysRevA.102.041302

Beams of cold and slow molecules from cryogenic buffer gas sources have played a central role in recent improved precision measurements [1,2], high-resolution spectroscopy [3,4], and the direct laser cooling and trapping of molecules at ultracold temperatures [5,6]. Direct cooling methods for molecules have the potential to produce a chemically diverse range of diatomic and polyatomic species at ultracold temperatures which are well suited for proposed applications including tests of fundamental physics [7], and controlled chemistry [8].

Cryogenic buffer gas beam sources rely on a flow of cold inert gas, usually helium or neon, to sympathetically cool the molecular species of interest and collapse the occupied rovibrational state distribution [9–12]. This thermalization takes place inside an enclosed cell as the species of interest becomes entrained within the inert gas flow and exits the cell through a small hole to form a beam. These molecular beams have forward velocities between ∼50 and 200 m/s and advances in slowing techniques using radiation pressure [13,14] have enabled molecules below ∼10 m/s to be captured and cooled by magneto-optical traps (MOTs) [15]. Today's molecular MOTs provide confining and damping forces comparable to those in atomic MOTs, but can only capture 10^4–10^5 molecules at densities up to $\sim 10^7$ cm^{-3} due to the low trappable flux and short loading times (∼20 ms) attainable when loading single pulses of molecules. While the first interactions between laser-cooled molecules were recently observed [16], many proposed applications require larger trapped samples at higher density and increasing the trappable flux remains a key challenge. More efficient slowing techniques are currently being pursued by multiple groups [17–21], and the production of brighter, slower molecular beams remains an active and complementary area of research [22–26].

This Rapid Communication presents a cryogenic source capable of producing bright, continuous beams of cold free radicals via laser ablation, thereby realizing a first step towards longer MOT loading times and the continuous accumulation of conservatively trapped dark-state molecules using an intermediate MOT stage. Our source uses helium buffer gas at 2.6 K and produces 20 ms duration pulses of molecules at repetition rates up to 55 Hz, limited by our ablation laser. To the best of our knowledge, these are the brightest time-averaged beams of free radicals reported from a helium buffer gas source and mark a demonstration of a continuous beam of cold free radicals.

The heart of our source is a two-stage pulse-tube refrigerator (Cryomech PT420) paired with a closed liquid helium reservoir [27] between the refrigerator's second stage and the cooled copper cell [Fig. 1(a)]. When cold, the reservoir contains ∼7 g (1.7 moles) of helium, which acts as a large thermal mass (heat capacity ∼16 J/K) to both dampen temperature oscillations from the refrigerator and allow the source to absorb high thermal loads from the ablation laser with limited heating. A constant source temperature is desirable to ensure reproducible molecular beam properties including flux, forward velocity, and rotational state distribution. We note that an equivalent thermal mass using copper alone at 2.6 K is impractical and would require cooling ∼400 kg of material. However, rare-earth alloy plates have been successfully used to dampen thermal oscillations in a similar manner [28]. While beneficial once cold, the closed helium reservoir leads to longer source cool-down and warm-up times. To counter this increase, our design limits the additional thermal mass to 6 kg of machined aluminum and copper parts, while largely replicating the source geometry of Ref. [10] [Fig. 1(b)]. Our design cools from 295 to 2.5 K in ∼2 hours and can warm up to 280 K in ∼4 hours, allowing rapid prototyping [Fig. 1(c)]. To help reduce warm-up times, we typically apply 0.5 W of 808 nm laser light to the cell to increase the liquid helium evaporation rate. At base temperature, the cell and the

*daniel.mccarron@uconn.edu

 ©2020 American Physical Society

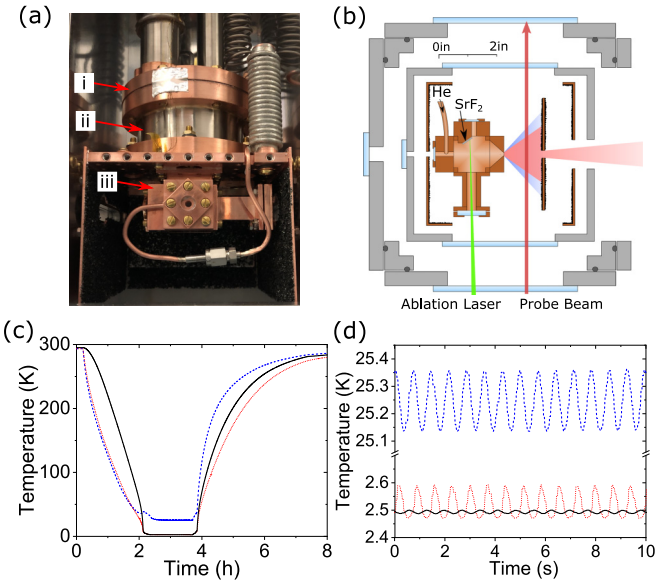

FIG. 1. Overview of the cryogenic source. (a) Photo of the source from behind, with the rear radiation shields removed to show (i) the refrigerator second stage, (ii) liquid helium reservoir, and (iii) cell. (b) Scale drawing of the source from above, showing the ablation and absorption beam paths. (c) Typical source cool-down and warm-up curves measured over several hours for the refrigerator first stage (dashed blue line), second stage (dotted red line), and cell (solid black line). (d) Short-term temperature stability for the same three regions as (c). Temperature oscillations at the 1.4 Hz period of the pulse-tube refrigerator are visible at all three regions.

refrigerator second stage are stable to ±5 and ±60 mK, respectively [Fig. 1(d)]. For reference, without the helium reservoir, the second-stage temperature stability is typically ±200 mK as the refrigerator pulses [29]. These larger oscillations have been reported to correlate with a ∼25% peak-to-peak variation in molecular beam flux [10], forcing several experiments to synchronize their repetition rates to the period of the pulse-tube refrigerator to recover reproducible pulses of molecules [3,13].

This work uses SrF molecules to characterize the source performance by ablating a SrF_2 target, mounted inside the cell at 30° relative to the molecular beam axis, using 15 mJ pulses of 532 nm light with 6 ns duration from a Nd:YAG laser. This light is tightly focused onto the surface of the target using a 200 mm focal length lens outside the vacuum chamber and the pulse energy is stable to within 1%. Cold helium buffer gas enters the cell through a fill line at the rear and exits through a conical face with a 40° half angle and a 3-mm-diameter aperture [Fig. 1(b)]. The typical helium buffer gas flow rate is 15 standard cubic centimeters per minute (sccm), equivalent to an in-cell steady-state helium density of 10^{16} cm^{-3} and a Reynolds number of ≈60. At this flow rate, the vacuum inside the cryogenic source chamber is 10^{-7} Torr, maintained by ∼700 cm^2 of cold charcoal cryopump. Throughout this work, a cold charcoal covered plate, containing a 6-mm-diameter hole, is positioned 34 mm in front of the cell exit aperture to reduce the helium gas load downstream [Fig. 1(b)]. Previous studies have shown that the location of this plate can strongly affect the molecular beam brightness [10,11].

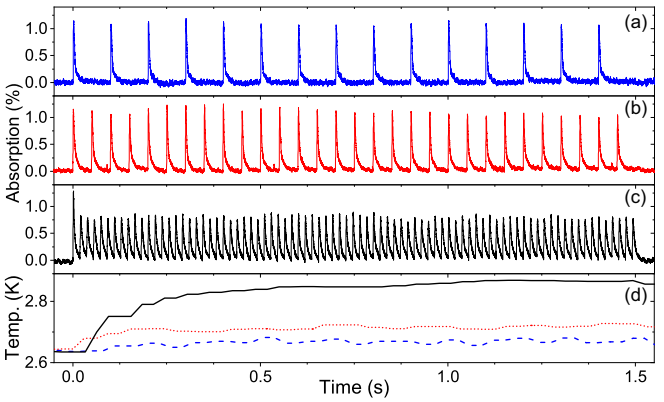

FIG. 2. Absorption and cell temperature traces measured over 1.5 seconds of source operation for ablation rates of (a) 10, (b) 20, and (c) 55 Hz. During these measurements, the source temperature (d) increased by 40 mK (dashed blue line), 80 mK (dotted red line), and 200 mK (solid black line), respectively. The time needed to cool back to 2.64 K was 1, 30, and 70 s for 10, 20, and 55 Hz operation, respectively.

Properties of the molecular beam are typically probed on the $X\,^2\Sigma(v=0, N=1)$ to $A\,^2\Pi_{1/2}(v'=0, J'=1/2)$ transition at 663 nm, using either absorption 20 mm downstream of the cell exit aperture or fluorescence detection 940 mm downstream. Upon exiting the cell, collisions boost the molecular beam forward velocity up to ≈140 m/s, with a FWHM of ≈50 m/s, approaching the forward velocity of the helium buffer gas (≈170 m/s) [12]. The molecular beam forward velocity was measured through the Doppler shift between two fluorescence profiles recorded using probe lasers transverse and counterpropagating to the molecular beam. The measured FWHM transverse velocity spread is 80 m/s, corresponding to a FWHM angular spread of 30°. The rotational temperature of the molecular beam is 1.0(2) K, measured by extracting the relative populations in $X\,^2\Sigma(v=0, N=0-4)$ using fluorescence signals from the $X\,^2\Sigma(v=0, N=0-4)$ to $A\,^2\Pi_{1/2}(v'=0, J'=1/2-9/2)$ transitions and calculated branching ratios to account for the varying line strengths [30]. Here molecules cool rotationally to below the cell temperature due to isentropic cooling near the cell aperture [31] and, at our rotational temperature, ≈50% of the molecules populate the $X\,^2\Sigma(v=0, N=1)$ state. These parameters are in agreement with measurements performed on a source with similar geometry [10].

To extract the number of molecules exiting the source in the $X\,^2\Sigma(v=0, N=1)$ state, we use the time integral of the resonant absorption signal, Doppler broadened absorption cross section [32], and assume a uniform density over the cross-sectional area of the molecular beam [10]. At ablation repetition rates of 1–2 Hz, where other helium buffer gas sources typically operate [10,33,34], the source produces 10^{11} molecules per steradian per pulse with negligible heating. We note that all reported numbers can vary by ≈ ±50%, depending on the spot ablated on the target. At ablation repetition rates of 10 and 20 Hz, the pulses of molecules are unchanged and the source produces 10^{12} and 2×10^{12} time-averaged molecules/sr/sec, respectively [Figs. 2(a) and 2(b)]. At 55 Hz, we consistently observe a ∼10% decrease in brightness (∝ the

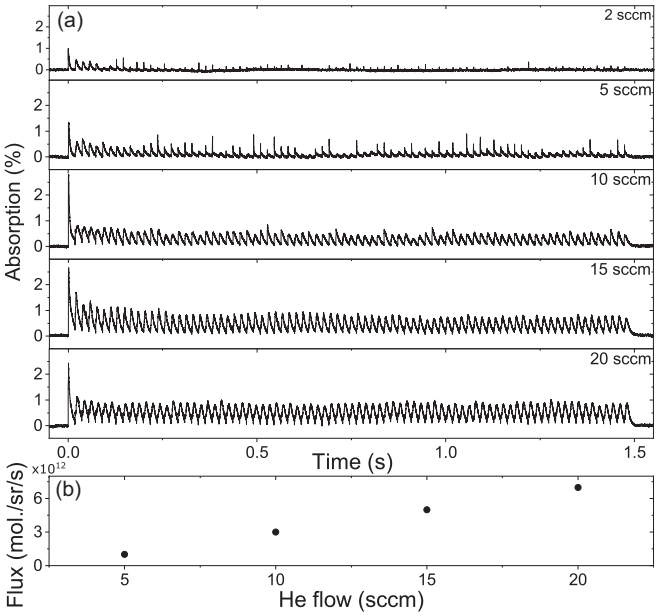

FIG. 3. Absorption vs helium buffer gas flow at a 55 Hz ablation repetition rate. (a) From top to bottom, the helium flow rates were 2, 5, 10, 15, and 20 sccm and the data are discussed in the text. These measurements were recorded in a random order using the same ablation spot on the target and highlight the temporary nature of the decrease in brightness measured over the first 2–5 pulses. (b) Time-averaged flux vs helium buffer gas flow rate for those flows that consistently produced pulses of molecules.

time-integrated absorption signal) over the first 2–5 pulses, with negligible change in rotational temperature, and typically produce 5×10^{12} molecules/sr/sec [Fig. 2(c)]. In-cell absorption measurements show that this initial decrease in brightness is correlated with decreasing in-cell molecular density and the extraction efficiency from the cell remains unchanged at ∼50%. This decrease in yield is temporary and a 100 ms pause in ablation pulses is sufficient to recover the original yield from the next pulse using the same ablation spot. This behavior is presumably due to heating within the cell, which increases by 40, 80, and 200 mK over 1.5 seconds of operation at 10, 20, and 55 Hz, respectively [Fig. 2(d)].

The successful production of bright, continuous beams of cold free radicals via ablation at 55 Hz depends critically on the helium buffer gas flow rate through the cell (Fig. 3). At flow rates of 2 and 5 sccm, the initial yield per ablation pulse is reduced by factors of 10 and 5, respectively, relative to our standard 15 sccm flow rate. We attribute this decrease to insufficient buffer gas density for complete thermalization. At 2 sccm, few molecules are detected in the beam after 250 ms of operation, while a flow of 5 sccm is sufficient to consistently produce pulses of molecules and realize 10^{12} molecules/sr/sec. Note that the sporadic spikes in Fig. 3(a) visible at flows of 2 and 5 sccm are ∼100 μs pulses of 10^8–10^9 molecules/sr and are not optical pickup due to the ablation laser. At flows of 10 sccm, we begin to continuously detect molecules exiting the cell with a brightness of 3×10^{12} molecules/sr/sec, increasing to 7×10^{12} molecules/sr/sec at 20 sccm. At 15 sccm, the beam brightness is typically modulated at 55 Hz by ∼80%, 20 mm downstream of the cell.

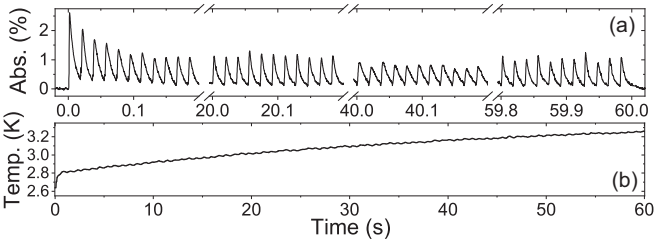

FIG. 4. A continuous beam of SrF molecules produced over 60 s showing (a) absorption and (b) the cell temperature. The mean brightness measured during this minute was $\sim 3 \times 10^{12}$ molecules/sr/sec and afterwards the cell required ∼2 minutes to cool back down to 2.6 K.

We project that this modulation will decrease to ∼60% a further 1.5 m downstream by convolving the measured molecular pulse temporal and velocity distributions.

The source performance is robust at 55 Hz for helium buffer gas flow rates $\geqslant$ 10 sccm, while a flow rate of $\geqslant$ 5 sccm is sufficient to sustain continuous operation at 10 and 20 Hz. Other groups using helium-based cryogenic sources typically use lower buffer gas flow rates, between 1–5 sccm [10,34–36], and several have reported erratic source behavior for ablation repetition rates >5 Hz [10,34]. We believe that these observations are due to insufficient helium flow and, other than the ablation pulse energy, we have found no other parameter that strongly affects beam brightness. Our source performance does not critically depend on the cell exit geometry; molecular beams with similar brightness were realized when the conical cell exit was replaced with a flat 0.5-mm-thick copper plate containing a 3-mm-diameter aperture. This lack of dependence on the cell exit geometry is in contrast to observations for a capillary fed cryogenic source [23]. Similar source performance was also realized for an elevated cell temperature of 4 K, after accounting for an increased rotational temperature of 2.0(3) K, which reduced the number of molecules in the $X\,^2\Sigma(v = 0, N = 1)$ state by ≈30%. This factor of 2 increase in rotational temperature highlights the importance of limiting heating during source operation to ensure reproducible beam properties. This source design has also proven to be straightforward to replicate and a second unit is now operational in our group and produces similar continuous beams of molecules.

As a demonstration of the stable and continuous nature of these molecular beams, we produce uninterrupted pulses of SrF molecules at 55 Hz over a 60 second duration using a buffer gas flow rate of 15 sccm (Fig. 4); this duration was chosen to avoid depleting an already heavily used target. During this time, the ablation spot was moved every ∼10 s to restore the decaying ablation yield and we measure a mean brightness of $\sim 3 \times 10^{12}$ molecules/sr/sec alongside a cell temperature increase of 0.6 K. Currently, the main limit on the continuous operation of our source is the durability of the ablated target and the challenge of continuously locating bright spots every ∼10 s. We speculate that considerably longer operation times would be within reach when using a new target and we typically replace targets after at least 10^6 pulses, which can correspond to a month of daily (but not continuous) use. Free radical production methods that ablate metals in the presence

a reactant gas (e.g., SF_6) have also been shown to produce brighter, more reproducible beams [34] and could potentially work well with our source design at high ablation repetition rates for longer durations. Our source design has sufficient cooling power for continuous operation at 55 Hz, which corresponds to ∼800 mW of incident power, and the cell reaches a steady-state temperature of 3.5 K after 5 minutes. Once at 3.5 K, we detect no evidence of liquid helium evaporation within the reservoir. By measuring the steady-state temperature versus incident power, we determine the temperature increase at thermal equilibrium to be ≈1 mK/mW of input power. Assuming a durable target is used, the absolute limit on operation time is set by saturation of the charcoal cryopump. In our design, a continuous flow of 15 sccm of helium can be maintained for 10 hours before saturation and this is readily extended by increasing the cryopump surface area.

In general, beams of molecules from helium buffer gas sources are preferable over neon-based beams for molecular laser cooling and trapping experiments due to their lower forward velocities, reduced divergence, and colder rotational temperatures [11,37]. Our source design combines these advantages alongside the ability to absorb high thermal loads with limited heating, similar to neon-based sources. We note that while the large thermal mass in our design slows heating, the maximum input power is determined by the cooling power of the pulse-tube refrigerator. In our setup, the maximum load is 2 W, permitting ablation repetition rates beyond 100 Hz and possible access to beams with more than 10^{13} molecules/sr/sec, similar to the brightest beams of free radicals from neon-based sources [12]. Currently, we cannot test ablation repetition rates beyond 55 Hz and it is unclear if higher-still helium flow rates will be necessary in this regime. At present, liquid helium fills ∼25% of the closed reservoir and increasing the helium mass would further improve the source temperature stability at the expense of longer cooldown and warm-up times. In principle, one could also pump on this reservoir to cool the source towards 1 K and produce colder, slower molecular beams, but with substantially reduced cooling power [37,38].

In summary, we have realized a robust cryogenic buffer gas source capable of producing continuous beams of cold free radicals via laser ablation with a time-averaged brightness of up to 7×10^{12} molecules/sr/sec in a single rovibrational state. The helium flow rate is the key parameter that determines the successful production of these beams via high repetition-rate ablation and must be ⩾10 sccm when ablating at 55 Hz. Our liquid helium reservoir is effective at stabilizing the cell temperature and slows heating during longer operation times, which ensures reproducible beam properties, although this feature is not essential. Our measurements show that the performance of our source does not critically depend on the cell temperature or exit geometry. This suggests that other groups currently using helium-based sources with smaller thermal masses could immediately realize brighter beams by using higher ablation repetition rates with sufficient buffer gas flow, provided that operation times are short to limit the effects of heating. These molecular beams represent a first step towards longer MOT loading times to trap larger samples at higher density and are well suited for continuous beam slowing and cooling techniques such as centrifugal deceleration [39,40], Zeeman slowing [21], and Zeeman-Sisyphus deceleration [18]. Note that the required molecular beam duty cycles in this new regime are currently unclear. Given the higher helium flow rates required for these beams, this progress will also likely demand measures to avoid an increased gas load in the MOT region, such as improved differential pumping and in-vacuum shutters on the beam axis [41]. For reference, today's molecular MOTs load single pulses of molecules over ∼20 ms. If similar loading times were used for atomic MOTs, only $\sim 10^5$–10^6 atoms would be trapped [42,43]. Given that typical molecular MOT lifetimes are short, ∼100 ms [5], the continuous accumulation of conservatively trapped molecules via an intermediate MOT stage is a particularly promising approach, a method which has been successfully demonstrated with chromium atoms [44]. These advances have the potential to increase the numbers and densities realized in laser-cooled samples of molecules by orders of magnitude and provide routine access to the molecule-molecule interactions required for many proposed applications.

Drawings of the machined parts needed to replicate this cryogenic source design and assembly instructions can be provided by contacting the corresponding author.

We thank D. DeMille and M. Steinecker for helpful discussions and J. Schnaubelt for carefully reading the manuscript. We acknowledge financial support from the NSF (CAREER Award No. 1848435) and the University of Connecticut, including a Research Excellence Award from the Office of the Vice President for Research.

[1] J. Baron, W. C. Campbell, D. DeMille, J. M. Doyle, G. Gabrielse, Y. V. Gurevich, P. W. Hess, N. R. Hutzler, E. Kirilov, I. Kozyryev, B. R. O'Leary, C. D. Panda, M. F. Parsons, E. S. Petrik, B. Spaun, A. C. Vutha, and A. D. West (The ACME Collaboration), Science **343**, 269 (2014).

[2] V. Andreev, D. G. Ang, D. DeMille, J. M. Doyle, G. Gabrielse, J. Haefner, N. R. Hutzler, Z. Lasner, C. Meisenhelder, B. R. O'Leary, C. D. Panda, A. D. West, E. P. West, and X. Wu (The ACME Collaboration), Nature (London) **562**, 355 (2018).

[3] E. B. Norrgard, E. R. Edwards, D. J. McCarron, M. H. Steinecker, D. DeMille, S. S. Alam, S. K. Peck, N. S. Wadia, and L. R. Hunter, Phys. Rev. A **95**, 062506 (2017).

[4] S. Truppe, S. Marx, S. Kray, M. Doppelbauer, S. Hofsäss, H. C. Schewe, N. Walter, J. Pérez-Ríos, B. G. Sartakov, and G. Meijer, Phys. Rev. A **100**, 052513 (2019).

[5] D. J. McCarron, J. Phys. B: At. Mol. Opt. Phys. **51**, 212001 (2018).

[6] M. R. Tarbutt, Contemp. Phys. **59**, 356 (2018).

[7] I. Kozyryev and N. R. Hutzler, Phys. Rev. Lett. **119**, 133002 (2017).

[8] N. Wells and I. C. Lane, Phys. Chem. Chem. Phys. **13**, 19036 (2011).

[9] S. E. Maxwell, N. Brahms, R. deCarvalho, D. R. Glenn, J. S. Helton, S. V. Nguyen, D. Patterson, J. Petricka, D. DeMille, and J. M. Doyle, Phys. Rev. Lett. **95**, 173201 (2005).

[10] J. F. Barry, E. S. Shuman, and D. DeMille, Phys. Chem. Chem. Phys. **13**, 18936 (2011).

[11] N. R. Hutzler, M. F. Parsons, Y. V. Gurevich, P. W. Hess, E. Petrik, B. Spaun, A. C. Vutha, D. DeMille, G. Gabrielse, and J. M. Doyle, Phys. Chem. Chem. Phys. **13**, 18976 (2011).

[12] N. R. Hutzler, H.-I. Lu, and J. M. Doyle, Chem. Rev. **112**, 4803 (2012).

[13] J. F. Barry, E. S. Shuman, E. B. Norrgard, and D. DeMille, Phys. Rev. Lett. **108**, 103002 (2012).

[14] S. Truppe, H. J. Williams, N. J. Fitch, M. Hambach, T. E. Wall, E. A. Hinds, B. E. Sauer, and M. R. Tarbutt, New J. Phys. **19**, 022001 (2017).

[15] J. F. Barry, D. J. McCarron, E. N. Norrgard, M. H. Steinecker, and D. DeMille, Nature (London) **512**, 286 (2014).

[16] L. Anderegg, L. W. Cheuk, Y. Bao, S. Burchesky, W. Ketterle, K.-K. Ni, and J. M. Doyle, Science **365**, 1156 (2019).

[17] D. DeMille, J. F. Barry, E. R. Edwards, E. B. Norrgard, and M. H. Steinecker, Mol. Phys. **111**, 1805 (2013).

[18] N. J. Fitch and M. R. Tarbutt, ChemPhysChem **17**, 3609 (2016).

[19] L. Aldridge, S. E. Galica, and E. E. Eyler, Phys. Rev. A **93**, 013419 (2016).

[20] X. Yang, C. Li, Y. Yin, S. Xu, X. Li, Y. Xia, and J. Yin, J. Phys. B: At., Mol. Opt. Phys. **50**, 015001 (2017).

[21] M. Petzold, P. Kaebert, P. Gersema, M. Siercke, and S. Ospelkaus, New J. Phys. **20**, 042001 (2018).

[22] E. P. West, A thermochemical cryogenic buffer gas beam source of ThO for measuring the electric dipole moment of the electron, Ph.D. thesis, Harvard University, 2017.

[23] V. Singh, A. K. Samanta, N. Roth, D. Gusa, T. Ossenbrüggen, I. Rubinsky, D. A. Horke, and J. Küpper, Phys. Rev. A **97**, 032704 (2018).

[24] D. Xiao, D. M. Lancaster, C. H. Allen, M. J. Taylor, T. A. Lancaster, G. Shaw, N. R. Hutzler, and J. D. Weinstein, Phys. Rev. A **99**, 013603 (2019).

[25] A. Jadbabaie, N. H. Pilgram, J. Kłos, S. Kotochigova, and N. R. Hutzler, New J. Phys. **22**, 022002 (2019).

[26] T. Gantner, M. Koller, X. Wu, G. Rempe, and M. Zeppenfeld, J. Phys. B: At. Mol. Opt. Phys. **53**, 145302 (2020).

[27] Temperature oscillation damping pot from Cryomech Inc.

[28] K. Allweins, L. M. Qiu, and G. Thummes, in *Advances in Cryogenic Engineering: Transactions of the Cryogenic Engineering Conference - CEC, Vol. 53*, edited by J. G. Weisend, J. Barclay, S. Breon, J. Demko, M. DiPirro, J. Patrick Kelley, P. Kittel, A. Klebaner, Al Zeller, M. Zagarola, S. Van Sciver, A. Rowe, J. Pfotenhauer, T. Peterson, and J. Lock, AIP Conf. Proc. No. 985 (AIP, New York, 2008), p. 109.

[29] Timothy Hanrahan (private communication).

[30] B. E. Sauer, J. Wang, and E. A. Hinds, J. Chem. Phys. **105**, 7412 (1996).

[31] H. Pauly, *Atom, Molecule, and Cluster Beams* (Springer, Berlin, 2000).

[32] D. Budker, D. F. Kimball, and D. P. DeMille, *Atomic Physics: An Exploration Through Problems and Solutions*, 2nd ed. (Oxford University Press, Oxford, 2008).

[33] G. Z. Iwata, R. L. McNally, and T. Zelevinsky, Phys. Rev. A **96**, 022509 (2017).

[34] S. Truppe, M. Hambach, S. M. Skoff, N. E. Bulleid, J. S. Bumby, R. J. Hendricks, E. A. Hinds, B. E. Sauer, and M. R. Tarbutt, J. Mod. Opt. **65**, 648 (2017).

[35] L. Anderegg, B. L. Augenbraun, E. Chae, B. Hemmerling, N. R. Hutzler, A. Ravi, A. Collopy, J. Ye, W. Ketterle, and J. M. Doyle, Phys. Rev. Lett. **119**, 103201 (2017).

[36] A. L. Collopy, S. Ding, Y. Wu, I. A. Finneran, L. Anderegg, B. L. Augenbraun, J. M. Doyle, and J. Ye, Phys. Rev. Lett. **121**, 213201 (2018).

[37] D. Patterson, J. Rasmussen, and J. M. Doyle, New J. Phys. **11**, 055018 (2009).

[38] C. Wang and B. Lichtenwalter, in *Advances in Cryogenic Engineering: Transactions of the Cryogenic Engineering Conference - CEC*, edited by J. G. Weisend, II, S. Breon, J. Demko, M. DiPirro, J. Fesmire, P. Kittel, A. Klebaner, J. Marquardt, G. Nellis, T. Peterson, J. Pfotenhauer, S. Yuan, M. Zagarola, and Al Zeller, AIP Conf. Proc. No. 1573 (AIP, New York, 2014), p. 1387.

[39] S. Chervenkov, X. Wu, J. Bayerl, A. Rohlfes, T. Gantner, M. Zeppenfeld, and G. Rempe, Phys. Rev. Lett. **112**, 013001 (2014).

[40] X. Wu, T. Gantner, M. Koller, M. Zeppenfeld, S. Chervenkov, and G. Rempe, Science **358**, 645 (2017).

[41] D. J. McCarron, M. H. Steinecker, Y. Zhu, and D. DeMille, Phys. Rev. Lett. **121**, 013202 (2018).

[42] X. Xu, T. H. Loftus, J. L. Hall, A. Gallagher, and J. Ye, J. Opt. Soc. Am. B **20**, 968 (2003).

[43] M. L. Harris, P. Tierney, and S. L. Cornish, J. Phys. B: At. Mol. Opt. Phys. **41**, 035303 (2008).

[44] P. O. Schmidt, S. Hensler, J. Werner, T. Binhammer, A. Görlitz, and T. Pfau, J Opt. B: Quantum Semiclass. Opt. **5**, S170 (2003).